Fast and Efficient in Silico 3D Screening: Toward Maximum Computational Efficiency of Pharmacophore-Based and Shape-Based Approaches

Johannes Kirchmair,[†] Stojanka Ristic,[†] Kathrin Eder,[†] Patrick Markt,[†] Gerhard Wolber,[‡] Christian Laggner,[†] and Thierry Langer*[,†,‡]

Department of Pharmaceutical Chemistry, Institute of Pharmacy and Center for Molecular Biosciences (CMBI), University of Innsbruck, Innrain 52, A-6020 Innsbruck, Austria, and Inte:Ligand Software-Entwicklungs- und Consulting GmbH, Clemens Maria Hofbauer-Gasse 6, A-2344 Maria Enzersdorf, Austria

Received January 24, 2007

In continuation of our recent studies on the quality of conformational models generated with CATALYST and OMEGA we present a large-scale survey focusing on the impact of conformational model quality and several screening parameters on pharmacophore-based and shape-based virtual high throughput screening (vHTS). Therefore, we collected known active compounds of CDK2, p38 MAPK, PPAR-γ, and factor Xa and built a set of druglike decoys using ilib:diverse. Subsequently, we generated 3D structures using CORINA and also calculated conformational models for all compounds using CAESAR, CATALYST FAST, and OMEGA. A widespread set of 103 structure-based pharmacophore models was developed with LigandScout for virtual screening with CATALYST. The performance of both database search modes (FAST and BEST flexible database search) as well as the fit value calculation procedures (FAST and BEST fit) available in CATALYST were analyzed in terms of their ability to discriminate between active and inactive compounds and in terms of efficiency. Moreover, these results are put in direct comparison to the performance of the shape-based virtual screening platform ROCS. Our results prove that high enrichment rates are not necessarily in conflict with efficient vHTS settings: In most of the experiments, we obtained the highest yield of actives in the hit list when parameter sets for the fastest search algorithm were used.

INTRODUCTION

3D virtual high throughput screening (vHTS) represents a potent state-of-the-art technique in drug discovery.[1] Structure databases containing precomputed conformational models show superior efficiency compared to approaches that treat the ligand as flexible during vHTS. Both techniques rely on the accurate representation of the bioactive conformation. With our recent studies on the quality of multiconformational models[2,3] we provided evidence that today's conformational model generators are able to calculate ensembles that represent the bioactive conformation with adequate accuracy for in silico screening most of the time. The quality of generated conformational ensembles was thereby evaluated by the assessment of the rmsd (root-mean-square deviation) between the bioactive conformation and the best fitting generated conformer. Investigations confirmed the common knowledge that the bioactive conformation may differ significantly from the global energy minimum conformation: The energetic threshold of protein-bound conformers often is located above the global energy minimum.[4−8] Therefore, the efficient and representative sampling of the low energy conformational space up to a certain maximum conformational energy threshold is an essential precondition for 3D vHTS. We showed in large-scale studies that conformational model generators work most accurately in terms of representing the protein-bound ligand conformation with energy cut off levels at about 20−25 kcal/mol.[2,3]

Although there is now a knowledge pool available on the quality of conformational model generators, hitherto there is only little information available on the impact of conformational ensemble accuracy on the results of pharmacophore-based and shape-based vHTS. Most of the knowledge on this issue originates from a few case studies (e.g., ref 9). Until now, there is no comparative large scale study available that provides significant statistical analysis on the impact of presampled conformational models on vHTS. Computational chemists are challenged in finding the best settings for screening: Not only do they reach for best enrichment but also they strive for maximum computational efficiency.

In this ongoing effort we now examine the impact of the quality of conformational models on the hit list obtained by different virtual screening protocols. We investigate the performance of pharmacophore-based and shape-based screening methods on four pharmaceutically highly relevant targets: CDK2, p38 MAPK, PPAR-γ, and factor Xa. The hit lists obtained by screening with 103 structure-based pharmacophore models and the corresponding 70 shape-based queries using ROCS[10,11] are examined in terms of several different quality criteria: sensitivity (Se), specificity (Sp), yield of actives (Y_a), enrichment (E), and the 'goodness of hits' (GH) score.[12]

All pharmacophore models were generated with LigandScout,[13,14] and CATALYST[15,16] was used as the screening platform. Dedicated multiconformational virtual libraries of

* Corresponding author phone: +43-512-507-5252; fax: +43-512-507-5269; e-mail: Thierry.Langer@uibk.ac.at.
[†] University of Innsbruck.
[‡] Inte:Ligand Software-Entwicklungs- und Consulting GmbH.

10.1021/ci700024q CCC: $37.00
Published on Web 10/11/2007

known active compounds and decoy molecules were calculated using the CATALYST catConf[2,3] module, the new CAESAR[17] algorithm, and OMEGA[3,4,7,18] using different conformational ensemble sizes. Both CATALYST screening modes (FAST vs BEST) and the fit value calculation procedures (FAST vs BEST) were analyzed. Therefore, we built an active compounds set for each investigated target and screened versus a druglike virtual compound collection designed with ilib:diverse.[19] The results and the performance of this approach is directly compared to the shape-based screening using OMEGA conformational models.

It has to be stressed that this study is not primarily investigating the generation of pharmacophore models optimized to obtain maximum yield of actives and/or sensitivity. We are in this case mostly interested in estimating the performance in an industrial environment and therefore avoided extensive manual refinement and optimization of the automatically derived pharmacophore models. However, we investigated the effects of using the information about binding site shapes and ligand shapes, since these two constraints can be rapidly applied to pharmacophore models. We consciously chose very heterogeneous pharmacophore model types in order to increase explanatory power and to avoid biasing: pharmacophore models with different features (e.g., hydrogen bond acceptors and hydrogen bond donors, positive ionizable features, ring aromatic features, and hydrophobic constraints) and models considering sterical constraints. Only applying such criteria ensures reliable performance analyses.

METHODS

Hardware Specifications and Runtime Environment. All operations considering calculation time were processed on a Intel Pentium Core 2 Duo 6400 PC equipped with 1 GB RAM running the Linux Fedora Core 6 operating system. A 15 nodes Linux PC cluster equipped with Intel Pentium IV and Intel Pentium Core 2 Duo 6400 processors was used for distributed computing.

Software Specifications. All settings differing from program defaults are mentioned explicitly in this paragraph. LigandScout 1.03 was used for pharmacophore model generation based on PDB[20] protein−ligand complexes; CATALYST 4.11 was used as the screening platform. All CATALYST parameters were kept default, except compare.minInterBlobDistance=0 (i.e., the minimum distance between features on a molecule required for it to be considered during compare/fit to a pharmacophore; enables tighter feature placements), FunctionMapping.Hydrophobe. Neighbor.numBondLessEqualFromOWithDoubleBond=0 (enables the fit of hydrophobic features to certain problematic phenyl sulfonamide moieties), and ViewDatabase.maxHits=10000 (maximum number of hits returned during screening). The CATALYST feature dictionary was kept default except for the application of the electrostatic fluorine-hydrogen bond donor interaction feature as published by Wolber et al.[13] Screening with ROCS 2.2 was performed with default settings. CAESAR (supplied with Pipeline Pilot 6.0.2.0), catConf (supplied with Pipeline Pilot 6.0.2.0), and OMEGA 2.0 conformational model generation were controlled by Pipeline Pilot[21] and Perl scripts. The ROC (receiver operating characteristic) curves have been elucidated with Pipeline Pilot and MS Excel (2002). Moreover, Pipeline Pilot was used for scaffold clustering and similarity analysis. Shell scripts and Perl were used for workflow automation. Screening runs were also performed with single conformer 3D structure databases built using CORINA[22−24] 3.00.

For clarity reasons, we abbreviate the settings for pharmacophore screening in CATALYST as follows: The number of maximally generated conformers per ensemble (1, 10, 20, 50, 100, and 250 conformations) prefixes the conformational model generator (CAESAR C, CATALYST FAST F, and OMEGA O) and the database search mode (FAST F, Best b). In this way, e.g., 050F-b stands for maximally 50 conformers per ensemble generated with CATALYST FAST and the BEST database search mode for screening. The fit value calculation method (needed for ROC curve analyses) was selected in concordance with the database screening mode: FAST database search implies usage of the FAST fit algorithm and BEST database search application of the BEST fit procedure. In concordance to this, we also abbreviate the ROCS screening settings: The number of maximally generated conformers per ensemble prefixes the conformational model generator and the minimum Tanimoto shape score (0.30, 0.40, 0.50, 0.55, 0.60, 0.65, 0.70, 0.75, 0.80, 0.85, 0.90). Therefore, 010O-065 stands for OMEGA conformational ensembles of maximally 10 conformers per compound and a Tanimoto similarity cutoff of 0.65.

Workflow. We subdivided our workflow into five major steps: (1) generation of compound sets, (2) pharmacophore model generation, (3) conformational model calculation and database generation, (4) in silico screening and scoring, and (5) data analysis.

(1) Generation of Compound Sets. *The Actives Sets.* Known biologically active lead structures of CDK2, p38 MAPK, and PPAR-γ were collected from the literature; in the case of factor Xa we used an in-house data set of lead structures in combination with ligands of protein−ligand complexes from the PDB. For each target, the 100 most diverse actives were determined by the Pipeline Pilot clustering protocol and subsequently used for the screening evaluation. Ligand structures that are part of the protein−ligand complexes used for the generation of pharmacophore models may be included in the actives sets in case they are cited in the literature and selected during the automated clustering process. The diversity of the test sets was assessed and quantified based on the number of structural clusters resulting from similarity analysis at a specific Tanimoto similarity threshold (Table 1). The actives sets comprise compounds of comparable molecular weight, number of rotatable bonds, number of hydrogen bond donors, and number of hydrogen bond acceptors. However, the ligand scaffolds of these targets differ. The ligand structures and literature references are available as Supporting Information.

The Inactives Set. ilib:diverse is a comprehensive fragment-based combinatorial chemistry program developed in Java. Its exhaustive algorithms allows the user to build very large compound libraries of highly diverse druglike or leadlike compounds.

ilib:diverse distinguishes between the user-adaptable priority reactivity and soft reactivity. Priority reactivity strictly

Table 1. Structural Dissimilarity of Active Compounds of the Test Sets and the Decoy Library[a]

similarity analysis [no. of clusters]	Tanimoto 0.7	Tanimoto 0.5
CDK2	14	29
p38 MAPK	4	17
PPAR-γ	26	72
factor Xa	16	55
inactives	672	8739

[a] The dissimilarity was assessed using Pipeline Pilot for clustering by maximum diversity, based on the Tanimoto coefficient. The more clusters formed at a certain Tanimoto coefficient value, the higher the diversity of the library. The data demonstrate that our test sets are highly diverse and well suited for screening investigations.

creates a prioritized atom list for each compound. If extensively used, this parameter completely destroys structure diversity. As a default value, every atom has a priority reactivity of 0. The atom reactivity editor allows the user to adjust the reactivity value for each atom in the range from −10 to +10. Apart from setting priorities, the druglikeness of the results can strongly be improved by creating a so-called trend reactivity. The idea behind soft reactivity is that the kind of combination ilib:diverse uses mostly resembles nucleophilic substitution. So, the electronegativity difference between an atom and its neighbors has been taken as a hint for slightly weighed preference. The selection of atoms with different soft reactivity values is implemented as follows: For a number of atoms with the same priority reactivity, an atom is chosen at random. If this atom's soft reactivity value is higher than 0, then it is selected for molecule generation. However, if this value is lower than 0, then probability of the atom to be eventually selected falls to 30%. For the remaining 70% of the cases, another random choice is started (including the current atom). ilib:diverse additionally features a comprehensive filter set for physicochemical property filtering and directed library generation. Besides basic organic groups also a focused so-called "pharm-group" containing well-known pharmaceutical scaffolds is available.

In the present study, ilib:diverse was used for the generation of a druglike library of decoys for the determination of the specificity and enrichment capability of pharmacophore-based virtual screening. Fragments in combination with a druglikeness filter were applied for the fast and efficient generation of a 10 000 compounds library. The fragment set includes, e.g., organic acids, alcohols, aliphatics, alkenes and alkynes, amides and imides, amines, amino acids, benzenes, esters, ethers, halogens, ketones and aldehydes, carbocycles, heterocycles, guanidines, nitriles, nitrogroups, oximes, and phosphor and sulfur containing groups. Moreover, the dedicated pharm-set features important pharmaceutically relevant scaffolds like, e.g., azepines, coumarines, tetracyclines. Physicochemical properties of the generated compounds were thereby restrained in order to obtain libraries that correspond to the active compound sets in terms of molecular weight, flexibility, the number of hydrogen bond acceptors, and hydrogen bond donors. Therefore, we analyzed the characteristics of the actives compound sets and adapted the ilib:diverse database generation settings in order to obtain compounds of comparable molecular properties. The molecules were assembled using four fragments per compound. A Gaussian distribution was applied on the number of rotors (mean 5, variance 6) and the compound size (mean 29, variance 29). Limits were applied for the number of hydrogen bond acceptors (2−9), the number of hydrogen bond donors (0−6), and the number of heteroatoms (maximally 8 nitrogens, 8 oxygens, or 5 halogens) per molecule. Stereocenters and double bond characteristics were assigned explicitly. The ilib:diverse reactivity filter was activated for the rejection of unstable molecules. These restraints allowed us to generate a well-defined focused library that is comparable to the active compounds set in the characteristics crucial for high quality decoys. We can therefore exclude that enrichment during vHTS is due to coverage of different property spaces. We are aware that a very few virtual compounds of this druglike inactives set may in real world have biological activity on the respective target. However, because of the low probability of activity the assumption that these compounds are in general inactive is a statistically adequate approximation (the hit rate in a random compound library is supposed to be located at about 0.1%; see ref 25). All ligand structures and the respective physicochemical properties are provided as Supporting Information.

(2) Pharmacophore Model Generation. All pharmacophore models were generated using LigandScout. This structure-based pharmacophore model generator is based on a sophisticated and customizable ligand−macromolecule complex interpretation algorithm. The software extracts and interprets ligands and their macromolecular environment from PDB files and automatically creates and visualizes advanced 3D pharmacophore models supporting multiple features per heavy atom to broaden the scope of a single model. A wide range of powerful editing tools lets the user generate customized, highly specific pharmacophores with little operating expense. Excluded volume recognition drastically increases specificity by considering sterical characteristics of the binding site. This fully automated procedure includes the following consecutive steps: (1) cleaning up the binding site of the protein (shows only amino acids within 7 Å distance from the ligand); (2) chemical feature recognition on the ligand side: hydrogen bond donor, hydrogen bond acceptor, positive ionizable, negative ionizable, hydrophobic, aromatic; (3) search for corresponding chemical features in the protein; (4) addition of the interaction feature to the model only if a reasonable protein−ligand interaction pair is found; and (5) addition of excluded volume spheres for opposite hydrophobic features in the protein.

LigandScout creates pharmacophore models that can be used in various external applications for virtual screening. However, these external software solutions have distinct needs for valid pharmacophore input. Hitherto, CATALYST does not support more than one feature per heavy atom. Therefore, we investigated literature of the respective protein−ligand complexes for reduction of the pharmacophores to versions that are compatible with CATALYST.

Our pharmacophore models are based on high-quality protein−ligand complexes of human origin. The vast majority of structures has resolution <2.5 Å; exceptions are marked with an '*' in Table 2. Both the binding site and the ligand were investigated for structural issues and cured manually. All pharmacophore models were generated with LigandScout in an automated way and subsequently exported for screening in CATALYST. Ahead of the actual screening

Table 2. List of All Pharmacophore Models Used in This Study: 48 CDK2, 36 Factor Xa, 4 p38 MAPK, and 15 PPAR-γ Pharmacophore Models

	queries[a]	binding site coat[b]	shape[d]	shared feature pharmacophore[c]
CDK2:1aq1	1	0	0	
CDK2:1ckp	1	0	0	
CDK2:1di8	1	0	0	
CDK2:1dm2	1	0	0	
CDK2:1e1v	1	0	0	
CDK2:1e9h	1	0	0	
				2x 1fvt-1ke6-1ke7-1ke8
CDK2:1fvt	10	3	0	2x 1fvt-1ke6-1ke8
CDK2:1g5s*	1	0	0	
CDK2:1gih*	1	0	0	
CDK2:1h00	2	0	0	
CDK2:1h07	1	0	0	
CDK2:1h08	1	0	0	
CDK2:1h1q	1	0	0	
CDK2:1jsv	1	0	0	
CDK2:1jvp	1	0	0	
CDK2:1ke5	1	0	0	
CDK2:1ke6	1	0	0	
CDK2:1ke7	1	0	0	
CDK2:1ke8	1	0	0	
CDK2:1ke9	1	0	0	
CDK2:1oiq	1	0	0	
CDK2:1oit	1	0	0	
CDK2:1p2a	1	0	0	
CDK2:1p5e	1	0	0	
CDK2:1pf8*	1	0	0	
CDK2:1pxm*	1	0	0	
CDK2:1pxn	1	0	0	
CDK2:1pxo	1	0	0	
CDK2:1pxp	1	0	0	
CDK2:1pye	1	0	0	
CDK2:1urw	1	0	0	
CDK2:1v1k	1	0	0	
CDK2:1vyw	1	0	0	
CDK2:1vyz	1	0	0	
CDK2:1w0x	1	0	0	
CDK2:1y8y	1	0	0	
CDK2:2bhe	1	0	0	
CDK2:2bhh*	1	0	0	
factor Xa:1f0r	1	0	0	
factor Xa:1f0s	3	0	0	2x 1f0s-1f0r
factor Xa:1fax*	2	0	0	
factor Xa:1g2m*	2	1	0	
factor Xa:1kye	1	0	0	
factor Xa:1lpg	1	0	0	
factor Xa:1lqd*	2	1	0	
factor Xa:1mq5	1	0	0	
factor Xa:1mq6	2	2	0	
factor Xa:1nfu	2	0	0	
				1nfx-1nfu
factor Xa:1nfx	3	0	0	1nfx-1nfw
factor Xa:1v3x	5	3	0	
factor Xa:1xka	1	0	0	
factor Xa:1xkb	5	3	0	
factor Xa:1z6e	1	0	0	
factor Xa:2bq7	1	0	0	
factor Xa:2cji	1	0	0	
factor Xa:2fzz	2	0	0	
p38:1a9u	1	0	0	
p38:1bl6	1	0	0	
p38:1bl7	1	0	0	
p38:1bmk	1	0	0	
PPAR-γ:1knu	3	3	2	
PPAR-γ:1nyx*	3	3	2	
PPAR-γ:1wm0*	1	0	1	
PPAR-γ:1zeo	2	2	1	
PPAR-γ:2fvj	1	0	1	
PPAR-γ:2g0h	1	1	1	
PPAR-γ:2prg	2	2	1	
PPAR-γ:4prg*	2	2	1	

[a] The table provides the overall number of pharmacophore models generated and used for screening derived from a certain X-ray structure. In some cases several different pharmacophore models are generated in order to achieve the best performance with CATALYST, most of the time due to CATALYST's lacking the ability to place more than one feature on a heavy atom. [b] Depicts the number of pharmacophores including the binding site coat (BSC). [c] The number of shared feature pharmacophores derived from a reference structure and one or more additional protein−ligand complexes. [d] CATALYST shape was introduced to pharmacophore queries. In particular for PPAR-γ pharmacophores we found well-defined binding coat and ligand shape definitions to significantly enhance performance.

process the successful fitting of the bioactive conformation of the ligand to the pharmacophore model was checked in order to ensure the recovery of this ligand by CATALYST screening. Fitting issues (e.g., very tight feature placement on adjacent heavy atoms may cause fitting problems) were cured manually by, e.g., feature deletion and/or feature sphere adaptation. Therefore, all pharmacophores at the very least fit the respective protein-bound ligand conformation.

As described above, LigandScout pharmacophores are in general based on a single protein−ligand complex. However, in the case of identical binding modes, several structure-based pharmacophores can be combined to a single, in general less restrictive but more profound shared feature pharmacophore model. This is a very useful approach if structural data are available for a series of compounds sharing one scaffold since it allows for the estimation of the importance of certain protein−ligand interactions: Identical interactions formed by several ligands are likely to be more important than features that are found in only one ligand. Especially in the case of 1fvt and the 1ke* series of X-ray structures the shared feature pharmacophore approach works very well (Table 2).

For comprehensive coverage of pharmacophore models we also investigated the performance of models using a binding site coat in order to simulate the shape of the protein. Thereby, small exclusion spheres are placed at the positions of every heavy atom of the protein site. Table 2 provides a list of all protein−ligand complexes investigated for pharmacophore model elucidation.

(3) Conformational Model Calculation and Database Generation. In our recent publications we proved that the conformational model generators OMEGA and CATALYST (both algorithm methods of the CATALYST catConf module, FAST and BEST) are able to predict the protein-bound ligand conformation in a quality that is suitable for virtual screening in the vast majority of all cases.[2,3] While CATALYST FAST works well for sampling of large databases, CATALYST BEST outperforms its more efficient counterpart especially when calculating very flexible or macrocyclic compounds with large conformational space. The superior accuracy of BEST has been confirmed by lower average rmsd values between the protein-bound ligand conformation and the best fitting generated conformer. Furthermore, 2D coordinate distribution plots based on the individual conformers aligned to the respective bioactive conformation using the pharmacophore-based alignment[14] integrated to LigandScout proves high diversity of conformational ensembles sampled by BEST. Nevertheless, FAST is clearly the first choice for vHTS, as BEST conformational search is fairly inefficient in terms of CPU time. OMEGA is an equivalent alternative to catConf; its accuracy and efficiency is in comparable range to FAST and well suited for vHTS. CAESAR (supplied with Pipeline Pilot) is a novel conformational model generator developed by Li et al.[17] that promises significantly increased efficiency. Today there are several efficient and reliable tools available for vHTS that replace BEST within the scope of vHTS. Thus, in this study on vHTS efficiency we focus on the performance of CAESAR, CATALYST FAST, and OMEGA.

All three conformational model generators were controlled using Pipeline Pilot in combination with Perl scripts.

Stereochemistry was considered during all steps of the workflow, and 3D information on the ligands was cut off in order to exclude biasing of the conformational sampling. With each model generator we calculated compound databases containing maximally 1, 10, 20, 50, 100, and 250 conformers per ensemble, respectively. Next, catDB was used to transfer these conformational models into CATALYST screening databases. The performance of pharmacophore-based screening was investigated using conformational models generated by all three conformational model generators; comparative screening with ROCS was examined using only the OMEGA conformational models. In addition, we also performed a pharmacophore screening run using CORINA 3D structure geometries in order to compare this very fast approach to the three conformational model generators.

(4) In Silico Screening and Scoring. *Pharmacophore Screening and Scoring.* Similar to both CATALYST's FAST and BEST algorithms for the conformational model generator tool catConf, there are also a FAST and a BEST flexible search mode available for database screening. FAST is focused on quick database screening; BEST is designed to provide high quality at reasonable speed. While FAST finds the best fit among existing conformers of the CATALYST database, BEST is able to further adapt these conformations to find more precise fittings. By default, this conformational change must not exceed an energy raise of 9.5 kcal. A hit during database screening is achieved by default, if at least one conformer of a compound matches all geometric feature constraints given by the pharmacophore model (e.g., location, excluded volume, angle, and distance).

CATALYST's fit value calculation represents a postprocessing tool to further increase enrichment similar to scoring functions used by docking approaches. Therefore, the fit value stands for the quality of the mapping of a compound to a pharmacophore model. In a reasonable structure-based and also ligand-based pharmacophore model, a compound with a high fit value is not necessarily highly active, but it is more likely to be active than a compound exhibiting a low fit value. The fit calculation process consists of the following four steps:

Initial Constraint Mapping. Only successfully checked compounds are considered during the subsequent mapping process.

Primary Feature Weight Summation. Weights for features without location constraints are summed up, provided that the features are present in the investigated compound.

Fitting. In the actual fitting step, the conformational model is searched for the best fitting conformer. The fit algorithm thereby determines the optimum orientations and highest fit values. Considering the deviation from the respective feature centers, the contributions of each feature are summed up.

Ranking of the Achieved Mappings. Two parameters determine the fit value: The feature mapping in context to the constraint centers and the respective feature weight. Feature weights enable the user to include the relative importance of individual features compared to others. The default feature weight of 1.0 is applied to features of any qualitative pharmacophore model (ligand-based as well as structure-based).

The fit value is calculated as follows

$$\text{Fit} = \sum W\left[1 - \sum\left(\frac{D}{T}\right)^2\right]$$

where W is the feature weight, D is the displacement from feature center, and T is the feature tolerance (location constraint sphere around feature center).

For the ROC curve analysis presented in this study, the GUI versions of FAST and BEST fit calculations were examined. There is another automated calculation option available in command line mode via the citest script when incorporated into a catEspDriver. However, to our knowledge and experience, the GUI version seems to be the best choice, since it was found and reported that the values obtained by both methods may differ slightly.[26]

ROCS Screening and Scoring. ROCS is a geometry-based screening technique that estimates similarity of compounds by analyzing the shape and volumes mismatch. Thereby, Gaussian terms represent the molecular volume, and these functions are used to minimize to the best global volume overlay. In this way, we used ROCS to compare the shape of bioactive conformation of the PDB compounds that have been considered for pharmacophore screening with the test sets compounds. The number of hits achieved during screening was analyzed with respect to the Tanimoto shape similarity cutoff used during the volume overlay process.

(5) Data Analysis. Data were elaborated with Perl and shell scripts.

PHARMACOLOGY AND TARGET SPECIFICATIONS

CDK2. Cyclin-dependent kinases (CDKs) are the catalytic subunit of heterodimeric serine/threonine protein kinases. They play an important role in the eukaryotic cell division cycle. Moreover, they are also involved in transcription and other processes.[27,28]

p38 MAP Kinase. The p38 mitogen-activated protein (MAP) kinase is a member of the stress-activated protein kinases (SAPK). p38 MAPK is therefore known as a stress-induced enzyme that is stimulated by, e.g., heat, UV light, lipopolysaccharides, proinflammatory cytokines, hormones, and high osmolarity.[29] p38 MAPK plays an important role in immune response: Downstream substrates like tumor necrosis factor-α (TNF-α), interleukin-6 (IL-6), cyclooxygenase-2 (COX-2), and interleukin-1 (IL-1) are regulated by the kinase.

PPAR γ. Expressed in the adipose tissue, PPAR-γ increases adipocyte differentiation, improves fatty acid storage, and enhances insulin sensitivity after agonist binding. The recently FDA approved PPAR-γ agonists, the thiazolidinediones, rosiglitazone, and pioglitazone, are used for the treatment of type 2 diabetes.[30]

Factor Xa. Factor Xa[31] represents a trypsin-like serine protease that catalyzes the conversion of prothrombin zymogene to its active form thrombin, which initiates the final stage of the blood coagulation pathway.

RESULTS AND DISCUSSION

We took efforts to constitute a highly diverse set of pharmacophore models to examine the impact of screening settings on the resulting hit lists. For screening in CATA-

Table 3. Average Conformational Model Size and Data File Size of the Inactives Data Set with Respect to the Conformational Model Generator Used for Sampling[a]

average conf model size	CAESAR	CATALYST FAST	OMEGA
inactives-001	1	1	1
inactives-010	7	8	10
inactives-020	15	16	18
inactives-050	41	38	39
inactives-100	80	66	65
inactives-250	185	117	109
data file size [megabytes]	**CAESAR**	**CATALYST FAST**	**OMEGA**
inactives-001	19	19	20
inactives-010	41	45	47
inactives-020	58	62	63
inactives-050	101	98	98
inactives-100	160	142	139
inactives-250	321	223	196

[a] The highest average number of conformers is achieved using CAESAR with a limit of maximally 250 conformers per ensemble.

LYST, the LigandScout pharmacophore models were adapted since LigandScout generates complex pharmacophore models with, e.g., multiple feature placements on one heavy atom of the ligand, which are not accepted by CATALYST. LigandScout therefore supplies a CATALYST compatibility mode for the generation of reduced pharmacophores. We evaluate several different user adaptable settings and algorithms and analyze the results using ROC curves. Moreover, we directly compare these results to the hit lists retrieved by ROCS screening in a dedicated section.

Basic Characteristics of the Conformational Models Used for Pharmacophore-Based Screening and Shape-Based Screening. The size of generated conformational models is the most important quality criterion for conformational ensembles: The larger the conformational model the more accurate the prediction and representation of the experimentally determined bioactive conformation.[2,3] With respect to the limit of maximally generated conformers per compound CAESAR, CATALYST FAST, and OMEGA in general produce a comparable amount of conformers per model. Significantly more conformations per ensemble are calculated with CAESAR in the case of a high limit of conformers per model (Table 3). However, within the range of small conformational models direct comparison of the quality and diversity of the models is feasible since these ensembles are of comparable size. For the in-depth analysis of the computing time needed for conformational model generation the reader is referred to our recent studies on CATALYST and OMEGA.[2,3]

Screening of LigandScout Pharmacophores Using CATALYST as Screening Platform. When running a vHTS experiment, one can evaluate several descriptors. The nature of the descriptor(s) to be evaluated and optimized will depend upon the final goal of the study. The following paragraphs will highlight some of these descriptors and present the evolution of these descriptors when varying the conformer generation and database mining parameters. For data analysis we used the ROC curves approach and enrichment indicators, as recently introduced into chemoinformatics by Triballeau[32] et al. which also describes the confusion matrix provided in Table 4.

Hit Size and Flexibility. Conformational model generators attempt to cover the large conformational space by a reasonable number of representative conformers. In our studies on conformational model generators[2,3] we examined the impact of increasing conformational space on the conformational ensemble quality in terms of representing the bioactive conformation. With increasing compound size and flexibility (partially reflected by the molecular weight and the number of rotors) conformational model generation becomes a more and more challenging problem. It was shown that the average rmsd between the best fitting generated conformer and the bioactive conformation increases significantly. Borodina et al. recently presented a model for the prediction of the conformational ensemble sizes necessary for the defined resolution of sampling of conformational space.[33]

Table 4. Classification of vHTS Hits

in silico \ in vitro	actives	inactives
selected	true positives (TP)	false positives (FP)
discarded	false negatives (FN)	true negatives (TN)

Table 5. Average Size of Compounds Obtained by Virtual Screening with Respect to the Conformational Model Size[a]

	FAST database search		BEST database search	
average hit size p38 MAPK 1a9u	MW	RB	MW	RB
inactives-020F	402	10	405	11
inactives-100F	402	11	406	12
inactives-250F	403	11	407	12
actives-020F	378	6	376	6
actives-100F	412	7	395	6
actives-250F	426	7	400	6

[a] As shown by the example of the p38 MAPK query of PDB complex 1a9u, conformational ensemble size and FAST/BEST database search mode have only marginal impact on the average size and flexibility of the compounds retrieved by virtual screening: both molecular weight and the number of rotatable bonds of the successfully fitted molecules do not increase with smoother coverage of conformational space.

Pharmacophore models innately consider a moderately restrained tolerance threshold formed spherically around the respective pharmacophore feature center; any successful placement of functional groups of a ligand within this tolerance sphere is considered as an adequate matching. Therefore, ensemble quality, within a certain range, seems to not be crucial for the matching of a compound to a pharmacophore model (Table 5).

Sensitivity. Sensitivity (Se) in the context of drug discovery (and vHTS) is a measure for the percentage of truly active compounds selected during screening: It is defined as the number of true positive compounds (TP) divided by the sum of true positives and false negatives (FN):

$$\mathrm{Se} = \frac{N_{\mathrm{selected\_actives}}}{N_{\mathrm{total\_actives}}} = \frac{\mathrm{TP}}{\mathrm{TP} + \mathrm{FN}}$$

Thus, Se 1 means that every active compound is retrieved during screening, while Se 0 means that no active compounds were selected.

Our results show rising Se with increasing conformational model size as well as with BEST flexible database search (compared to its FAST counterpart): While one conformer per compound and FAST database search show an average sensitivity of 0.08, the computationally most ex-

Table 6. Demands in CPU Power with Respect to the Fastest Screening Setup[a]

average search time	FAST database search	BEST database search	ROCS
inactives-001O	1	15	11
inactives-010O	4	55	55
inactives-020O	7	89	100
inactives-050O	13	166	208
inactives-100O	21	240	325
inactives-250O	29	318	555

[a] BEST database search of compounds with maximally 250 conformers per ensemble takes 318 times more CPU time than screening of compounds with one conformer per ensemble using the FAST database search mode. The BEST database search mode is about 10−15 times slower than its FAST counterpart and therefore comparable with the performance of ROCS.

pensive settings (250 conformers per ensemble, BEST database search) achieve a five times higher value (Table 7). Since we are using highly diverse pharmacophore model sets for all investigated targets, of course the standard deviations are very high (Table 11). However, the trend toward increasing Se with higher demands in calculation time is distinctive.

There is no front-runner beneath the three conformational model generators; all products perform mainly similar. CAESAR seems to be best suited for the sampling of CDK2 ligands, CATALYST FAST for PPAR-γ, and OMEGA for p38 MAPK, respectively. CDK2 and p38 MAPK pharmacophores have an about 1.5 times higher sensitivity than PPAR-γ and factor Xa queries. The 3D structure generator CORINA produces only a single 3D structure per compound. Compared to single conformers calculated with CAESAR, CATALYST FAST, and OMEGA, CORINA obtains a comparable percentage of actives in the hit list, yet CORINA is significantly faster than the conformational model generators.

The highest impact of the screening setup on Se is achieved for PPAR-γ and factor Xa. The PPAR-γ pharmacophore queries obtain lower sensitivity, which is caused by the increased specificity of the models by introducing binding site coats and ligand shapes. In the case of factor Xa the highly selective positive ionizable feature (interaction with ASP189) included in several queries is responsible for lower average sensitivity; the fraction of factor Xa inhibitors that do not comprise a positive ionizable area are omitted by these models.

Specificity. Specificity (Sp) is a measure for the fraction of truly inactive compounds being correctly rejected during vHTS. Sp is defined as the number of TN divided by the sum of TN and FP:

$$\mathrm{Sp} = \frac{N_{\mathrm{discarded\_inactives}}}{N_{\mathrm{total\_inactives}}} = \frac{\mathrm{TN}}{\mathrm{TN} + \mathrm{FP}}$$

Thereby, Sp 0 defines the worst-case scenario where all inactives are selected by error as actives, whereas Sp 1 means all inactives rejected.

Table 8 depicts the average Sp values. Neither increasing model size, nor smoother sampling of conformational space, nor BEST flexible database search have a favorable impact on this quality characteristic: Average Sp drops from 1.00 with one conformer per molecule using FAST database screening to 0.91 with 250 conformers per molecule using BEST database screening. The decrease of Sp is more prominent with the BEST screening algorithm. Models of all three conformational model generators show very similar behavior; the average Sp of p38 MAPK, PPAR-γ, and factor Xa are well comparable. However, we find a higher dependency of Sp on the screening setup with the CDK2 pharmacophores, where the average Sp drops from 0.99 to 0.87 with increasing computational demands. This behavior can be easily explained since the CDK2 models are the softest-defined models among all queries of this study. While active compounds are able to successfully fit the pharmacophore model with only a very few calculated conformations, the probability of successful matching of inactive compounds increases with smoother sampling of conformational space and, even more, with further fit optimization by the BEST screening algorithm. Considering these results we can conclude that Sp drops with higher computational efforts particularly for moderately restrained pharmacophore models, while well-defined pharmacophore queries are not affected significantly. This means that with more exhaustive conformational search and BEST flexible screening more inactive compounds are wrongly selected as being active during vHTS. The Sp standard deviations are given in Table 11.

Yield of Actives. The yield of actives (Y_a) measures the fraction of the known actives in the hit list. It is defined as follows

$$Y_a = \frac{\mathrm{TP}}{n}$$

where TP is the number of known actives in the hit list, and n is the number of compounds in the search list, respectively.

A trend toward lower Y_a with increasing computational efforts (i.e., larger conformational samples, more exhaustive conformational search, and BEST flexible search) can be deduced from Table 9: Compared to ensembles of maximally 10 conformers the increase in conformational ensemble size to maximally 250 conformers drops Y_a from an average of 0.31−0.18. The BEST flexible search algorithm demonstrates an even more developed negative impact on Y_a: While single conformer screens achieve Y_a 0.23 on average, the 250 conformers per ensemble setup drops Y_a to 0.11.

No significant difference in the performance of the three conformational model generators can be detected. Yet, OMEGA shows favorable performance for p38 MAPK, which is balanced by the lower Y_a with factor Xa pharmacophores. The 3D structures generated by CORINA show very good or even best Y_a during virtual screening, together with the single conformers calculated with OMEGA.

Most of the factor Xa pharmacophore models comprise a positive ionizable feature. Since this feature is less common in druglike molecules (compared, e.g., to hydrogen bond features or hydrophobic moieties), this constraint enables factor Xa queries to achieve the highest Y_a of all four investigated targets. Thereby, best performance is achieved using conformational models of maximally 10−20 conformers per ensemble. In contrast to that, PPAR-γ shows only a moderate, yet constant Y_a. The PPAR-γ models are depend-

Table 7. Average Se Achieved with All Pharmacophore Queries of a Certain Target with Respect to Screening Setup[a]

fast DB screen	CORI-F	001C-F	001F-F	001O-F	010C-F	010F-F	010O-F	020C-F	020F-F	020O-F
CDK2	0.17	0.13	0.13	0.13	0.25	0.23	0.20	0.28	0.25	0.22
p38 MAPK	0.18	0.10	0.10	0.22	0.20	0.15	0.30	0.23	0.17	0.30
PPAR-γ	0.01	0.01	0.01	0.01	0.05	0.05	0.05	0.08	0.10	0.07
factor Xa	0.03	0.03	0.03	0.02	0.11	0.11	0.10	0.16	0.15	0.10
average	0.10	0.07	0.07	0.10	0.15	0.14	0.16	0.19	0.17	0.17

fast DB screen	050C-F	050F-F	050O-F	100C-F	100F-F	100O-F	250C-F	250F-F	250O-F
CDK2	0.31	0.27	0.25	0.33	0.29	0.26	0.34	0.30	0.27
p38 MAPK	0.26	0.22	0.32	0.27	0.24	0.33	0.30	0.26	0.35
PPAR-γ	0.14	0.15	0.13	0.18	0.19	0.18	0.25	0.25	0.24
factor Xa	0.22	0.20	0.19	0.26	0.23	0.22	0.31	0.26	0.28
average	0.23	0.21	0.22	0.26	0.24	0.25	0.30	0.27	0.28

best DB screen	CORI-b	001C-b	001F-b	001O-b	010C-b	010F-b	010O-b	020C-b	020F-b	020O-b
CDK2	0.24	0.20	0.20	0.20	0.32	0.30	0.27	0.37	0.33	0.30
p38 MAPK	0.24	0.21	0.21	0.28	0.25	0.25	0.34	0.29	0.30	0.36
PPAR-γ	0.04	0.03	0.03	0.04	0.11	0.13	0.11	0.19	0.23	0.18
factor Xa	0.06	0.08	0.08	0.06	0.16	0.17	0.15	0.23	0.21	0.15
average	0.14	0.13	0.13	0.15	0.21	0.21	0.22	0.27	0.27	0.24

best DB screen	050C-b	050F-b	050O-b	100C-b	100F-b	100O-b	250C-b	250F-b	250O-b
CDK2	0.40	0.36	0.33	0.42	0.38	0.35	0.44	0.39	0.35
p38 MAPK	0.33	0.34	0.39	0.34	0.37	0.41	0.37	0.39	0.42
PPAR-γ	0.33	0.32	0.30	0.40	0.41	0.36	0.48	0.48	0.43
factor Xa	0.31	0.29	0.27	0.35	0.33	0.31	0.40	0.35	0.37
average	0.34	0.33	0.32	0.38	0.37	0.35	0.42	0.40	0.39

[a] For example, the average Se of all CDK2 models using maximally 20 CAESAR conformers per ensemble and CATALYST's fast screening algorithm is 0.28. Se increases with rising computational efforts in vHTS: more exhaustive conformational model generation and database search retrieves considerably more active compounds.

Table 8. Specificity (Sp) Drops with Increasing Demands in Computational Resources[a]

fast DB screen	CORI-F	001C-F	001F-F	001O-F	010C-F	010F-F	010O-F	020C-F	020F-F	020O-F
CDK2	0.99	0.99	0.99	0.99	0.97	0.96	0.96	0.95	0.95	0.95
p38 MAPK	1.00	1.00	1.00	1.00	0.99	0.99	0.99	0.99	0.99	0.99
PPAR-γ	1.00	1.00	1.00	1.00	0.99	0.99	0.99	0.99	0.99	0.99
factor Xa	1.00	1.00	1.00	1.00	0.99	0.99	0.99	0.99	0.99	0.99
average	1.00	1.00	1.00	1.00	0.99	0.99	0.99	0.98	0.98	0.98

fast DB screen	050C-F	050F-F	050O-F	100C-F	100F-F	100O-F	250C-F	250F-F	250O-F
CDK2	0.94	0.93	0.94	0.92	0.92	0.93	0.91	0.90	0.93
p38 MAPK	0.98	0.98	0.99	0.98	0.98	0.98	0.97	0.97	0.98
PPAR-γ	0.98	0.98	0.98	0.98	0.97	0.98	0.96	0.96	0.97
factor Xa	0.98	0.98	0.98	0.97	0.98	0.98	0.97	0.97	0.97
average	0.97	0.97	0.97	0.96	0.96	0.97	0.95	0.95	0.96

best DB screen	CORI-b	001C-b	001F-b	001O-b	010C-b	010F-b	010O-b	020C-b	020F-b	020O-b
CDK2	0.97	0.97	0.97	0.97	0.94	0.93	0.93	0.92	0.91	0.91
p38 MAPK	0.99	0.99	0.99	0.99	0.98	0.98	0.98	0.97	0.97	0.97
PPAR-γ	0.99	0.99	0.99	0.99	0.98	0.98	0.98	0.97	0.96	0.97
factor Xa	0.99	0.99	0.99	0.99	0.98	0.97	0.97	0.96	0.96	0.96
average	0.99	0.99	0.99	0.99	0.97	0.97	0.97	0.95	0.95	0.95

best DB screen	050C-b	050F-b	050O-b	100C-b	100F-b	100O-b	250C-b	250F-b	250O-b
CDK2	0.88	0.88	0.89	0.87	0.86	0.88	0.85	0.84	0.87
p38 MAPK	0.95	0.95	0.96	0.94	0.93	0.94	0.92	0.92	0.94
PPAR-γ	0.94	0.94	0.95	0.93	0.92	0.93	0.91	0.90	0.92
factor Xa	0.95	0.95	0.95	0.94	0.94	0.94	0.93	0.93	0.94
average	0.93	0.93	0.93	0.92	0.91	0.92	0.90	0.90	0.92

[a] More inactives are selected during virtual screening runs with hardware demanding setups compared to runs with high-speed screening settings.

ing on a profound definition of the binding site shape and also the ligand shapes because the pharmacophoric feature constraints itself are not restrictive enough for reliable screening: The majority of the PPAR-γ queries consist of only a few hydrophobic interaction spheres (which of course are rather unspecific) and one or two hydrogen-bonding features. As a consequence, the average Y_a for this target is only moderate yet relatively constant throughout all screening setups (which is likely to be caused by the ligand shape included in these pharmacophore models). In between these two query classes there are located the p38 MAPK models, which show a very high average Y_a when screening single

Table 9. Yield of Actives (Y_a) in the Hit List Is Considerably Higher for Low Quality Conformational Models and FAST Database Screening[a]

fast DB screen	CORI-F	001C-F	001F-F	001O-F	010C-F	010F-F	010O-F	020C-F	020F-F	020O-F
CDK2	0.36	0.36	0.36	0.37	0.34	0.30	0.29	0.28	0.26	0.24
p38 MAPK	0.52	0.30	0.30	0.52	0.26	0.19	0.30	0.21	0.14	0.24
PPAR-γ	0.16	0.12	0.12	0.18	0.15	0.15	0.15	0.13	0.16	0.14
factor Xa	0.28	0.36	0.36	0.22	0.43	0.44	0.32	0.43	0.42	0.26
average	0.33	0.28	0.28	0.32	0.30	0.27	0.27	0.26	0.24	0.22

fast DB screen	050C-F	050F-F	050O-F	100C-F	100F-F	100O-F	250C-F	250F-F	250O-F
CDK2	0.24	0.21	0.20	0.21	0.19	0.19	0.18	0.16	0.17
p38 MAPK	0.14	0.11	0.18	0.11	0.09	0.15	0.09	0.08	0.13
PPAR-γ	0.12	0.12	0.14	0.12	0.12	0.13	0.11	0.11	0.13
factor Xa	0.38	0.38	0.37	0.36	0.35	0.34	0.33	0.32	0.34
average	0.22	0.21	0.22	0.20	0.19	0.20	0.17	0.17	0.19

best DB screen	CORI-b	001C-b	001F-b	001O-b	010C-b	010F-b	010O-b	020C-b	020F-b	020O-b
CDK2	0.27	0.24	0.24	0.28	0.22	0.19	0.18	0.18	0.16	0.14
p38 MAPK	0.28	0.23	0.23	0.29	0.17	0.13	0.16	0.10	0.09	0.11
PPAR-γ	0.11	0.08	0.08	0.11	0.10	0.09	0.08	0.10	0.11	0.08
factor Xa	0.28	0.34	0.34	0.25	0.32	0.32	0.28	0.29	0.28	0.23
average	0.23	0.22	0.22	0.24	0.20	0.19	0.18	0.17	0.16	0.14

best DB screen	050C-b	050F-b	050O-b	100C-b	100F-b	100O-b	250C-b	250F-b	250O-b
CDK2	0.13	0.12	0.12	0.12	0.11	0.10	0.10	0.09	0.09
p38 MAPK	0.07	0.06	0.08	0.05	0.05	0.07	0.04	0.04	0.06
PPAR-γ	0.09	0.09	0.09	0.08	0.08	0.08	0.08	0.08	0.08
factor Xa	0.26	0.26	0.25	0.24	0.24	0.25	0.23	0.22	0.24
average	0.14	0.13	0.13	0.12	0.12	0.13	0.11	0.11	0.12

[a] The fastest settings obtain highest Ya.

Table 10. GH Score Comprises Y_a, Se, and Sp[a]

fast DB screen	CORI-F	001C-F	001F-F	001O-F	010C-F	010F-F	010O-F	020C-F	020F-F	020O-F
CDK2	0.31	0.30	0.30	0.31	0.32	0.28	0.26	0.27	0.25	0.23
p38 MAPK	0.43	0.25	0.25	0.45	0.25	0.18	0.30	0.22	0.14	0.25
PPAR gamma	0.12	0.09	0.09	0.14	0.13	0.12	0.13	0.12	0.14	0.12
factor Xa	0.22	0.27	0.27	0.17	0.35	0.36	0.26	0.36	0.35	0.21
average	0.27	0.23	0.23	0.27	0.26	0.24	0.24	0.24	0.22	0.20

fast DB screen	050C-F	050F-F	050O-F	100C-F	100F-F	100O-F	250C-F	250F-F	250O-F
CDK2	0.25	0.22	0.20	0.23	0.20	0.20	0.20	0.18	0.19
p38 MAPK	0.17	0.13	0.21	0.14	0.13	0.19	0.14	0.12	0.18
PPAR gamma	0.12	0.13	0.14	0.13	0.14	0.14	0.14	0.14	0.15
factor Xa	0.33	0.33	0.32	0.33	0.32	0.31	0.32	0.30	0.32
average	0.22	0.20	0.22	0.21	0.20	0.21	0.20	0.19	0.21

best DB screen	CORI-b	001C-b	001F-b	001O-b	010C-b	010F-b	010O-b	020C-b	020F-b	020O-b
CDK2	0.25	0.22	0.22	0.26	0.24	0.21	0.19	0.21	0.19	0.17
p38 MAPK	0.27	0.22	0.22	0.29	0.19	0.16	0.20	0.14	0.14	0.17
PPAR gamma	0.09	0.06	0.06	0.09	0.10	0.10	0.09	0.12	0.13	0.11
factor Xa	0.22	0.28	0.28	0.20	0.28	0.28	0.24	0.27	0.26	0.20
average	0.21	0.20	0.20	0.21	0.20	0.19	0.18	0.19	0.18	0.16

best DB screen	050C-b	050F-b	050O-b	100C-b	100F-b	100O-b	250C-b	250F-b	250O-b
CDK2	0.18	0.16	0.16	0.17	0.15	0.15	0.16	0.14	0.14
p38 MAPK	0.13	0.13	0.15	0.11	0.12	0.14	0.11	0.12	0.14
PPAR gamma	0.14	0.14	0.14	0.15	0.16	0.14	0.16	0.16	0.16
factor Xa	0.26	0.26	0.25	0.26	0.25	0.25	0.26	0.24	0.26
average	0.18	0.17	0.17	0.17	0.17	0.17	0.17	0.16	0.17

[a] The data prove that settings for higher conformational ensemble quality and more demanding screening do not imply better vHTS results: most of the time, fast setups perform better than expensive setups.

conformer databases, and the CDK2 queries, which start from a little below 0.40 and drop down to about 0.10 using the most demanding computational settings. For all investigated targets, the maximum Y_a values are obtained using conformational models that do not exceed 10 conformers per ensemble (Tables 9 and 12). As already pointed out for the sensitivity of the models, also in the case of Y_a the standard deviations are very high due to the highly diverse pharmacophore model sets (Table 11).

Enrichment. The performance and goodness of pharmacophore models can be meaningfully evaluated by enrichment assessment. The parameter measures the increase of actives in the hit list with respect to random search. It is defined by the Y_a, the number of actives in the database (A),

Table 11. Average Standard Deviations for Se, Sp, and Y_a with All Screening Setups

STDEV pharmacophore screening	Se	Sp	Y_a
CDK2	0.26	0.11	0.26
p38 MAPK	0.17	0.01	0.12
PPAR gamma	0.08	0.03	0.09
factor Xa	0.15	0.06	0.28
average	0.16	0.05	0.19

STDEV ROCS screening	Se	Sp	Y_a
CDK2	0.09	0.07	0.10
p38 MAPK	0.07	0.02	0.09
PPAR gamma	0.08	0.11	0.15
factor Xa	0.06	0.05	0.16
average	0.08	0.06	0.12

Table 12. Screening Setups for Highest Y_a[a]

highest Y_a	pharmacophores		ROCS	
CDK2	001O-F	0.37	020O-085	0.20
p38 MAPK	001O-F	0.52	050O-090	0.64
PPAR gamma	001O-F	0.18	100O-080	1.00
factor Xa	010F-F	0.44	250O-085	0.72

[a] Average value obtained by all pharmacophore/ROCS queries of a certain target.

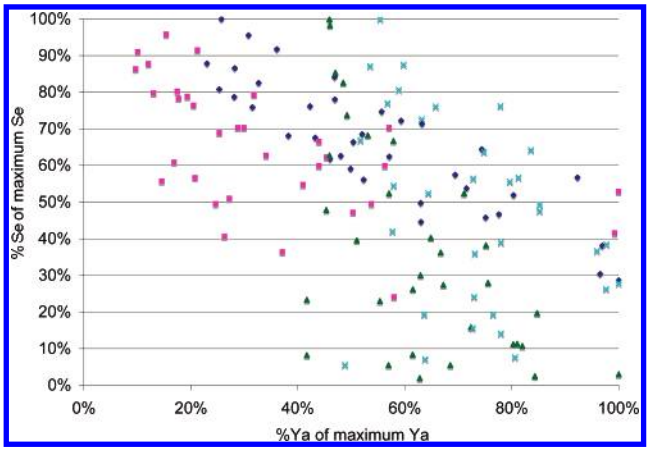

Figure 1. Average Y_a and sensitivity achieved by the screening of CDK2 (blue), p38 MAPK (magenta), PPAR-γ (green), and factor Xa (turquoise) lead structures in dependence on the pharmacophore screening setup. The *x*-axis illustrates the percentage of Y_a achieved with a certain setup with respect to the maximum; the *y*-axis depicts the percentage of sensitivity obtained with respect to the maximum sensitivity of all screening runs. The data points of the best performing software settings are located preferably close on the upper right side of the diagram (i.e., maximum Y_a and maximum Se).

and the total number of entries (N) as follows:

$$E = \frac{Y_a}{A/N}$$

An issue of the enrichment factor is the high dependence on the number of actives and inactives in the test database.[32] In our study we therefore scaled all screening runs by using actives test sets of exactly 100 actives for every target and the 10 000 inactives set. Thus, $E = Y_a \times 101$. Since only the relation of the number of actives to the number of inactives discriminates Y_a from E we provide all data on enrichment as Supporting Information. Most of our pharmacophore models generated with LigandScout show impressive enrichment; CDK2, factor Xa, and thrombin models perform excellently. The average enrichment for all screening setups is 21 for CDK2, 17 for p38, 11 for PPAR gamma, and 31 for factor Xa.

Goodness of Hit List. Besides a pool of other very useful measures for pharmacophore model and screening quality, the GH score represents a quality measure particularly designed for quality assessment of pharmacophore models. Weight is thereby shifted toward the retrieval of a high value of actives:

$$\mathrm{GH} = \left(\frac{3}{4} Y_a + \frac{1}{4} \mathrm{Se}\right) \times \mathrm{Sp}$$

It is a very useful adaptation because of the fact that databases may contain compounds that bind in alternative binding modes, at different binding sites, or may act at an allosteric center that of course cannot be selected by the pharmacophore model. The GH score is a valuable tool to sum up most of all of the effects seen above, since it is based on the examination of sensitivity and specificity. Table 10 provides data on the decrease of hit quality with rising computational cost. The trends are similar to those observed for enrichment, except for PPAR-γ, where a slight trend toward higher hit scores with more demanding computational settings can be deduced.

Best Performing Screening Setups. The analysis of several descriptors for the quality of virtual screening provides an overview on the characteristics and importance of different screening parameters. However, the question, which screening setup performs best in general is very delicate; it cannot be answered objectively and is highly dependent on the aims of a screening campaign. In the case of limited resources for in vitro testing of new lead structure candidates the screening of huge virtual libraries requires highly constrained models that are able to obtain maximum enrichment rates. From the data presented above it is obvious that in this case small conformational models of the screening compounds and the FAST screening algorithm are likely to show favorable performance compared to setups that require higher computational power. On the other side, in industrial scale computational chemists may aim at the coarse prefiltering of virtual compounds before high-throughput biological testing and may therefore shift the focus from enrichment to sensitivity. If comprehensive hit lists are requested, large conformational models and extensive screening algorithms may be preferred. Overall, models showing both high Y_a and high sensitivity are most promising for screening campaigns. However, this will always be a tradeoff between both parameters, and the decision on where to put the focus remains up to the modeler (Figure 1).

ROC Curve Analysis of Pharmacophore Screening Runs. Receiver operating characteristic (ROC) curve analysis is a potent technique for investigating the ability of screening protocols to discriminate between active and inactive compounds.[32] Thereby, the true positive rate is plotted against the false positive rate. On such a graph, a random search of structures would be represented as a diagonal rising from the origin of the upper right corner; a ROC curve above this diagonal demonstrates the ability of a certain screening setup to correctly discriminate between active and inactive com-

Table 13. Characteristics of Individually Investigated Pharmacophore Models[a]

target	PDB	setup	% Se		% Sp		$\%Y_a$		features	protein residues involved in H-bonding
CDK2	1fvt-1ke6-1ke7-1ke8 shared feature pharmacophore	10	78	90	93	83	11	5	1 HBA	LEU83
		20	83	93	90	75	8	4	1 HBD	GLU81
		50	85	95	84	66	5	3	2 HP	
		250	93	96	77	57	4	2		
p38	1a9u + BSC	10	31	40	100	99	53	31	2 HBA	LYS53, MET109
		20	32	42	99	98	33	19	1 RA	
		50	37	46	99	97	16	12	2 HP	
		250	42	51	98	94	17	7		
PPAR-γ	1knu + SHAPE + BSC	10	4	7	100	100	21	13	2 HBA	HIS323, TYR473
		20	9	18	100	99	32	21	1 RA	
		50	15	27	100	99	31	18	3 HP	
		250	22	47	99	98	23	18		
Factor Xa	1f0r	10	8	16	100	99	29	15	2 HBA	GLY219
		20	15	28	100	98	33	14	1 HBD	ASP189
		50	21	38	99	97	25	10	1 RA	
		250	35	51	99	94	19	8	1 HP	

[a] Abbreviations: hydrogen bond donor (HBD), hydrogen bond acceptor (HBA), ring aromatic feature (RA), hydrophobic area (HP), ligand shape (SHAPE), and binding site coat (BSC).

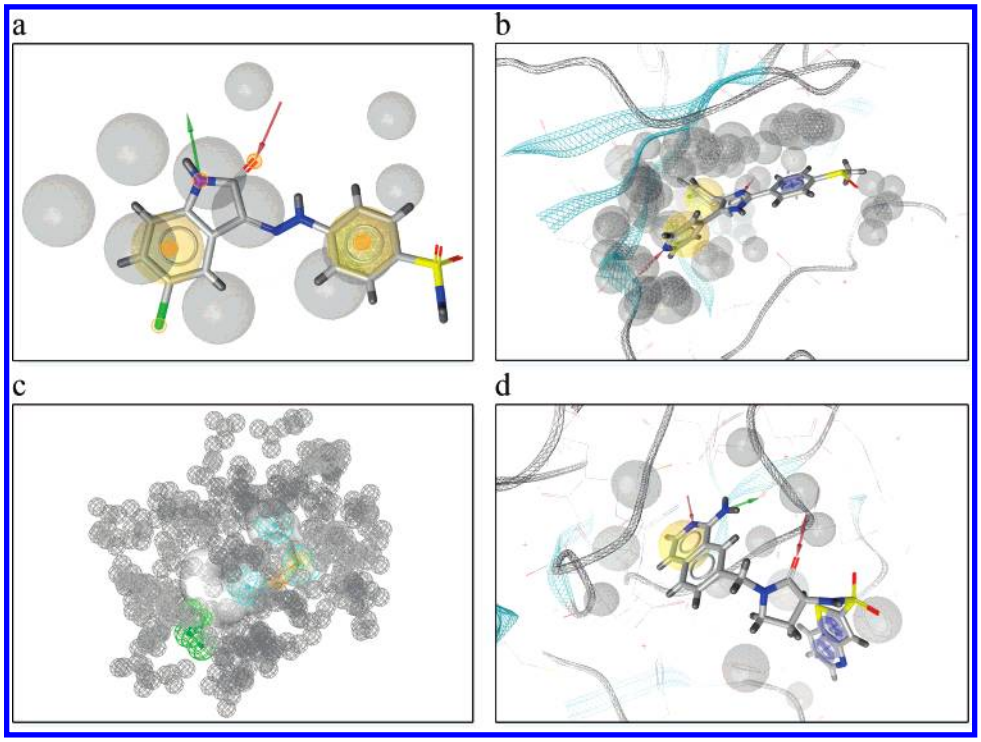

Figure 2. Pharmacophore models used for ROC curve analysis. The images provide an insight on the characteristics of the models and illustrate the usage of binding site coats and ligand shapes. The illustrations show the simplified LigandScout pharmacophore models that are suitable for in silico screening with CATALYST. Images (a), (b), and (d) were rendered using LigandScout: positive ionizable feature (blue sphere), negative ionizable feature (red sphere), ring aromatic/hydrophobic feature (yellow sphere), hydrogen bond acceptor (red vector), hydrogen bond donor (green vector), and excluded volume spheres (gray sphere). Screenshot (c) is taken from DS Visualizer, which depicts the model using a CATALYST shape around the ligand. Feature code with DS Visualizer: ring aromatic feature (orange sphere), hydrophobic feature (turquoise sphere), hydrogen bond acceptor (green sphere), and excluded volume spheres (gray sphere). More detail on the composition of the models is given in Table 13.

pounds. The curve of an ideal screening campaign would skyrocket vertically to the upper-left corner and then continue to the upper-right corner.

For ROC curve analysis we selected one pharmacophore model per target, each representing a certain pharmacophore model type: (1) 1fvt, 1ke6, 1ke7, and 1ke8-ls4, shared feature pharmacophore model; (2) 1a9u, pharmacophore model comprising a binding site coat (BSC) using small excluded volume spheres placed on every heavy atom of the protein; (3) 1knu, pharmacophore model including a ligand shape and binding site coat; and (4) 1f0r, basic LigandScout pharmacophore model comprising a positive ionizable feature.

The characteristics of these pharmacophore models including the definition of abbreviations are given in Table 13; the pharmacophore models analyzed using ROC curves are presented in Figure 2. Figure 5 presents the ROC curves of the search queries. From these diagrams it becomes obvious that Se increases in correlation to the calculated conformers per compound: The more conformers per compound the more active compounds are retrieved during virtual screening. Thereby, using BEST database screening instead of its FAST

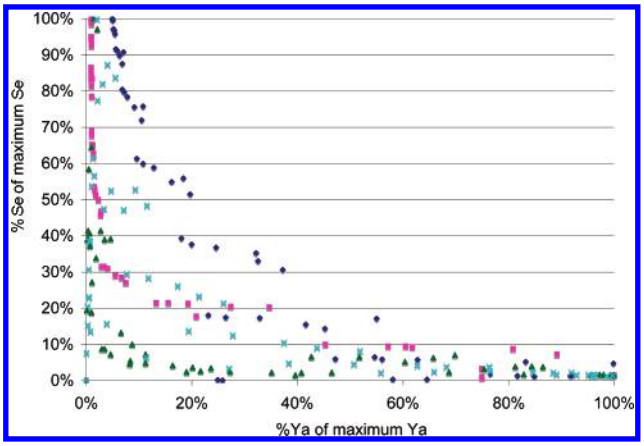

Figure 3. Average Y_a and sensitivity achieved by screening for CDK2 (blue), p38 MAPK (magenta), PPAR-γ (green), and factor Xa (turquoise) lead structures in dependence on the ROCS screening software setup (cp. Figure 1).

counterpart shows even more impact on Se with respect to conformational model size. However, with increasing Se the steepness of the curve, the distance from random search is reduced (e.g., in the case of the 1fvt-1ke6-1ke7-1ke8 shared feature query): Higher enrichment and/or earlier recognition of the inhibitors is obtained when using small conformational models and the FAST screening algorithm. In order to increase the number of hits retrieved from screening switching from FAST to BEST screening mode is more convenient than upsizing the number of conformers per molecule since this avoids the conformational recalculation of the database. In the case of 1a9u the screening process performs significantly better when using the BEST database search and the BEST fitting algorithm (compared to the FAST counterparts). This is likely to be caused by the binding site coat applied of this query. Since this extension is so far rather uncommon in pharmacophore queries, it may not have been considered during the development and optimization of the CATALYST search algorithm.

The factor Xa query of PDB complex 1f0r is a good example to demonstrate the advantages of using several pharmacophore models for the description of a binding pocket: In the case of 1f0r the ligand is interacting with ASP189 via H-bonds. Thus, this pharmacophore model comprises the respective H-bond feature of the aromatic amino group. However, a large part of known factor Xa inhibitors shows a positive ionizable group at this protein anchor. The generation and usage of two different pharmacophore models considering the H-bond network and positive ionizable area, respectively, assures reliable Se and Y_a at the same time.

Shape-Based Screening Using ROCS As Screening Platform. We analyzed the performance of Openeye's ROCS using their conformational model generator OMEGA. The major screening parameter within the ROCS is the Tanimoto shape similarity. This setting defines the minimum shape similarity of a compound to a query structure in order to be considered as a hit: The higher the Tanimoto similarity index, the higher of the shape similarity of the hits. Therefore, Tanimoto similarity cutoff 0.3 means that almost every active

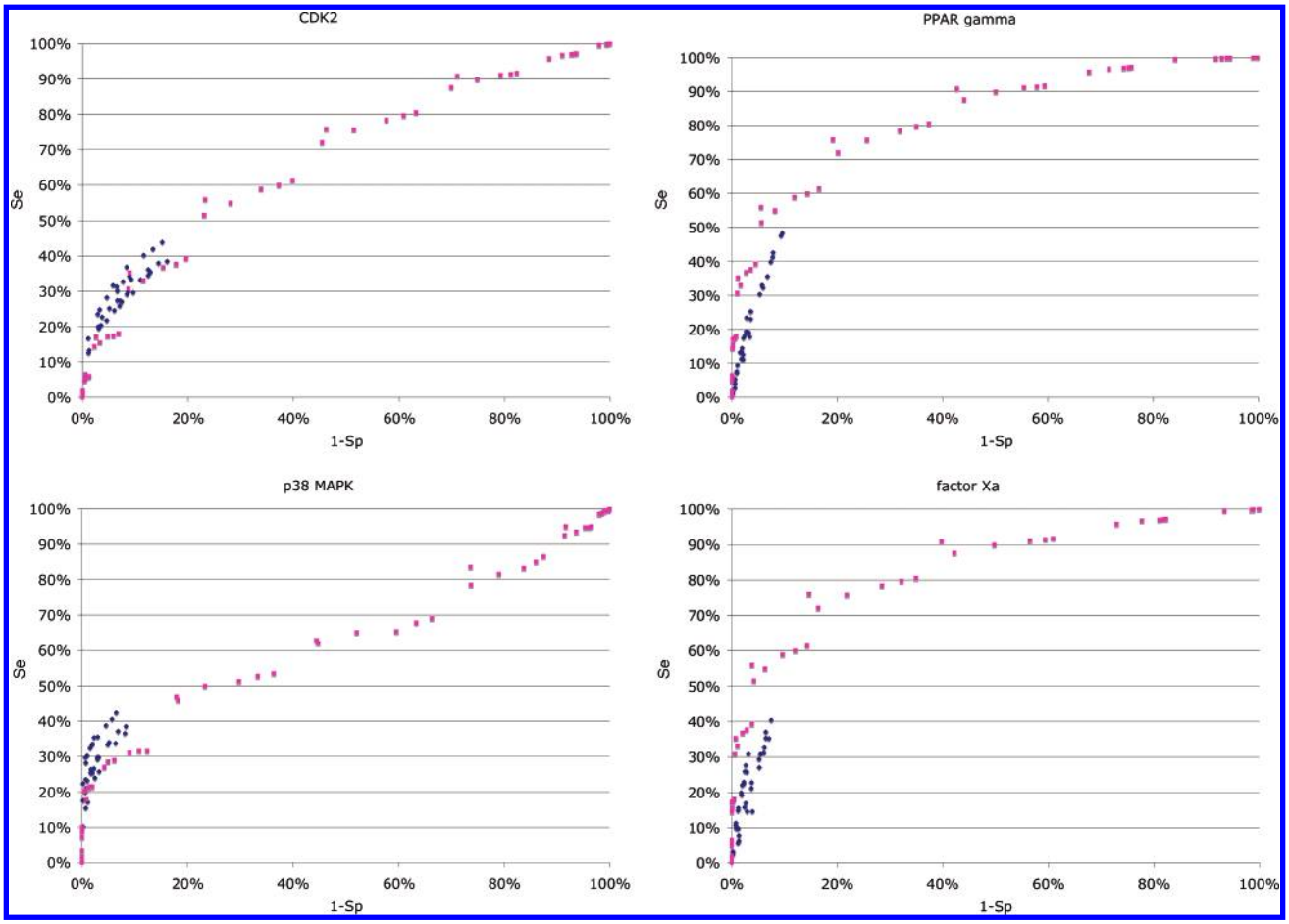

Figure 4. Comparison of the screening performance of pharmacophore model setups (blue) and ROCS runs (magenta). An ideal screening filter would achieve Se = 100% and 1-Sp = 0%. The nearer the data points are to the upper-left corner the better the screening protocol.

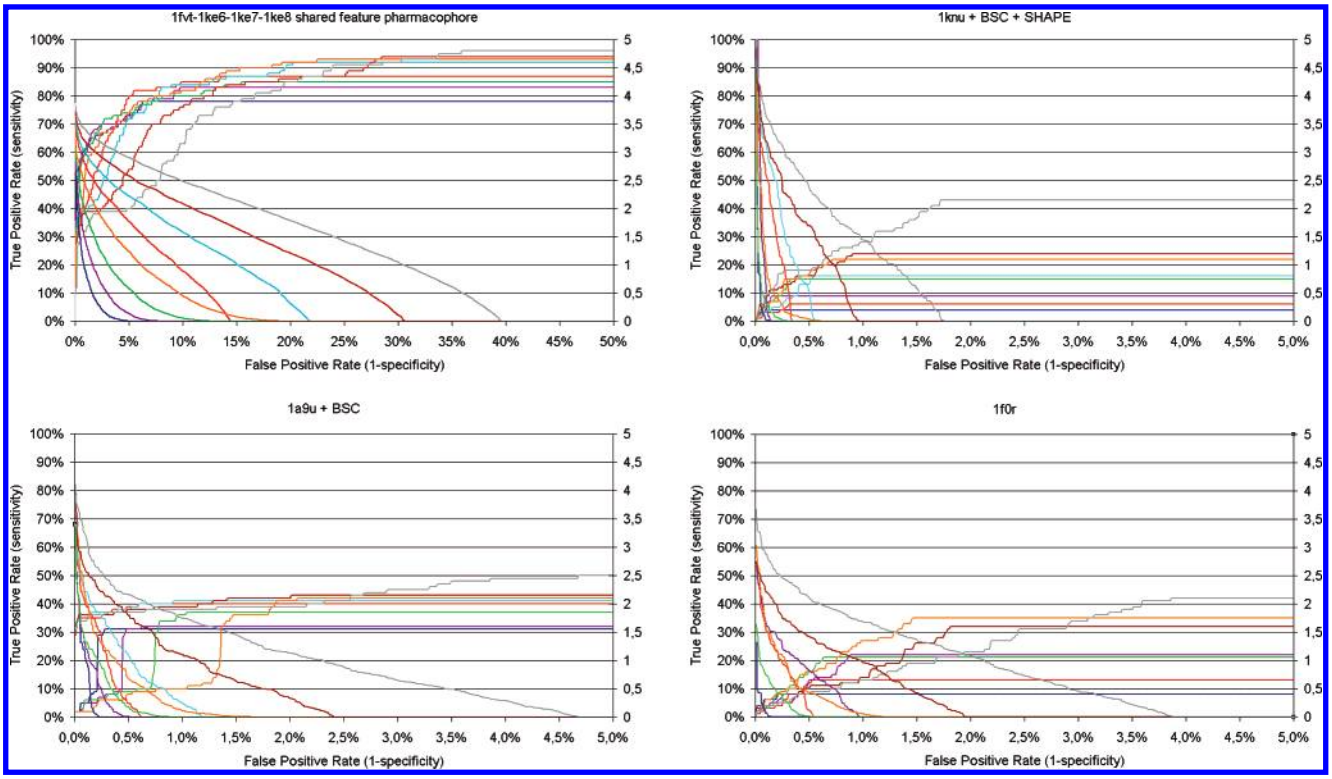

Figure 5. ROC curves illustrate the efficiency and reliability of different search setups. The true positive rate is plotted on the primary *y*-axis, the fit values are applied on the secondary *y*-axis, and the false positive rate is assigned to the *x*-axis. For clarity, the same colors for the true positive rate and the respective score are used: values of the primary *y*-axis ascend with increasing false positive rate, fit values descend on the secondary *y*-axis with increasing false positive rate. Color code: 010F-F (blue), 010F-b (red), 020F-F (violet), 020F-b (turquoise), 050F-F, (green), 050F-b (brown), 250F-F (orange), and 250F-b (gray). Despite concerns on comparability issues of the diagrams shown, we decided to extract only the most interesting *x*-axis part, in order to resolve the differences between screening settings; a uniform *x*-axis scale for all diagrams would mask interesting observations. The corresponding raw data on all ROC curves are available as Supporting Information.

compound is recognized during screening, even when screening a database with only one conformer per ensemble but of course at the expense of specificity and enrichment. In general, a similarity cutoff above 0.9 is too restrictive and obtains only a very few hits; the optimum setting is located within these extremes, as shown below. Data on sensitivity and specificity are provided as Supporting Information.

Yield of Actives. In contrast to pharmacophore screening the overall Y_a increases with the number of conformers per ensemble: The more complex the conformational models the higher the Y_a. The factor Xa queries obtain maximum Y_a with 250 conformers per model, the PPAR-γ queries with 100 conformers per model, p38 MAPK queries with 50 conformers per ensemble, and CDK2 with 20 conformers per model, respectively. This observation can in part be explained by looking at the flexibility of the ligands: Factor Xa and PPAR-γ compounds comprise more rotatable bonds than the p38 MAPK and CDK2 ligands. Thus, for ROCS screening of flexible ligands a comprehensive coverage of conformational space increases hit quality. The standard deviations are provided in Table 11, and the setups for highest Y_a for all four investigated targets are given in Table 12.

Enrichment. As pointed out above, the enrichment can be directly derived from the Y_a by considering the number of actives and inactives in the test database(s). Therefore, we provide these data only as Supporting Information.

The Best Performing ROCS Screening Setup. Defining the best performing screening setup for ROCS is even more difficult than for pharmacophore screening since in the case of ROCS the larger spreading between Se and Y_a provide even more space for optimization. Of course, with ROCS high Y_a or maximum sensitivity can be obtained, but like for pharmacophore screening this is always a tradeoff between both parameters (Figure 3).

Pharmacophore-Based Screening vs Shape-Based Screening. *Screening Speed.* Computational efforts are not an issue when screening a small compound set on a single target as, e.g., carried out in this study. However, demands in computational power become a serious issue when screening up to several millions of compounds. In particular for the recently introduced parallel screening and/or counter screening approaches, high efficiency is an absolutely essential prerequisite.[34−36] As demonstrated in Table 6 by the analysis of the screening times of all CDK2 models and the inactives data set, careful selection of screening parameters (conformational model size, CATALYST FAST/BEST database screening mode) can save computational power in the range of 100 or even more. The comparison of the screening speed between CATALYST and ROCS is quite delicate since CATALYST uses an indexing system to prefilter the vast majority of molecules that do not satisfy all pharmacophoric features requested by a certain query. So the actual number of compounds to be screened in 3D space is much lower for CATALYST than for ROCS. The

consideration of partial pharmacophore mappings is likely to overthrow this ratio.

Screening Quality. Similar to ROC curves, Figure 4 illustrates the performance of all pharmacophore (blue dots) and ROCS (magenta dots) screening setups with respect to the average Se and Sp. While pharmacophore models show favorable performance in the case of CDK2 and p38 MAPK, ROCS screening achieves better results with PPAR-γ and factor Xa.

For the experimental verification of the activity of virtual screening hits the absolute number of compounds selected during screening is decisive for the complexity of biological testing. Hence, lacking specificity may soon get an issue, and for most of all of the screening campaigns, in vitro tests exceeding 10−20% compounds of the total library are not reasonable. In the most interesting range of specificity in particular pharmacophore models obtain very good results with several different screening setups. Overall, both methods show only very narrow differences in terms of screening accuracy.

CONCLUSIONS

We present a large-scale study on the impact of several screening parameters on the hit list quality of pharmacophore-based and shape-based virtual screening. One hundred three structure-based pharmacophore models were developed using LigandScout and evaluated in terms of the quality of the hit lists obtained from screening with CATALYST. Therefore, databases comprising conformational ensembles of the test compounds were calculated using CAESAR, CATALYST FAST, and OMEGA. We found that these three conformational model generators produce conformational models of comparable quality. Increasing computational efforts in both conformational model generation (i.e., increasing conformational model size) and database screening (FAST vs BEST CATALYST screening algorithm) retrieve more active compounds during virtual screening. However, specificity of softer-constrained pharmacophore models drops significantly; as a direct consequence also the yield of actives is diminished. Therefore we recommend using CATALYST databases with a limit of maximally 50 generated conformers per ensemble and FAST generation algorithm combined with FAST database search as the default pharmacophore screening setup. In the case of very restrictive pharmacophores, more exhaustive generator and search settings can be used to achieve more hits. On average, increasing conformational model size is the better choice than using BEST instead of FAST database search. However, the first case implies costly recalculation of already existing databases. BEST flexible database search is likely to decrease the yield of actives and to raise computational costs multiple times—which should be carefully considered particularly for parallel screening. In contrast to pharmacophore screening, the shape-based screening platform ROCS is more dependent on comprehensively sampled conformational models. While the first approach achieves highest Y_a with very small conformational ensembles, the latter one tends to increase accuracy with larger conformational models, which of course demands more computational power during both conformational sampling and screening. The best ROCS results were obtained with a Tanimoto shape similarity index between 0.80 and 0.90. We want to recommend computational chemists to assess the quality of screening protocols using ROC curve analysis since this technique allows one to easily investigate and optimize screening performance.

The best performing screening setup depends largely on the focus of a screening campaign (compound library size, capacity for biological testing, etc.). Overall, we provide evidence that efficient resource management not only saves computational power but also may improve the performance of screening protocols.

ACKNOWLEDGMENT

We thank the Inte:Ligand Computer Science, Software and Algorithms Group Vienna for excellent LigandScout and ilib: diverse software support.

Supporting Information Available: Structural data, physicochemical property distributions, and literature references on the actives and inactives compounds sets, the enrichment factors obtained by different virtual screening setups, and data on Se, Sp, and enrichment factors of ROCS screening. This material is available free of charge via the Internet at http://pubs.acs.org.

REFERENCES AND NOTES

(1) Hoffmann, R. D.; Meddeb, S.; Langer, T. Use of 3D pharmacophore models in 3D database searching. In *Computational Medicinal Chemistry for Drug Discovery*; Tollenaere, J., De Winter, H., Langenaeker, W., Bultinck, P., Eds.; Dekker, Inc.: New York, 2004; pp 461−482.

(2) Kirchmair, J.; Laggner, C.; Wolber, G.; Langer, T. Comparative analysis of protein-bound ligand conformations with respect to Catalyst's conformational space subsampling algorithms. *J. Chem. Inf. Model.* **2005**, *45*, 422−430.

(3) Kirchmair, J.; Wolber, G.; Laggner, C.; Langer, T. Comparative performance assessment of the conformational model generators Omega and Catalyst: a large-scale survey on the retrieval of protein-bound ligand conformations. *J. Chem. Inf. Model.* **2006**, *46*, 1848−1861.

(4) Boström, J. Reproducing the conformations of protein-bound ligands: a critical evaluation of several popular conformational searching tools. *J. Comput.-Aided Mol. Des.* **2001**, *15*, 1137−1152.

(5) Boström, J.; Norrby, P.-O.; Liljefors, T. Conformational energy penalties of protein-bound ligands. *J. Comput.-Aided Mol. Des.* **1998**, *12*, 383−396.

(6) Nicklaus, M. C.; Wang, S.; Driscoll, J. S.; Milne, G. W. A. Conformational changes of small molecules binding to proteins. *Bioorg. Med. Chem.* **1995**, *3*, 411−428.

(7) Perola, E.; Charifson, P. S. Conformational analysis of drug-like molecules bound to proteins: an extensive study of ligand reorganization upon binding. *J. Med. Chem.* **2004**, *47*, 2499−2510.

(8) Vieth, M.; Hirst, J. D.; Brooks, C. L., III Do active site conformations of small ligands correspond to low free-energy solution structures? *J. Comput.-Aided Mol. Des.* **1998**, *12*, 563−572.

(9) Toba, S.; Srinivasan, J.; Maynard, A. J.; Sutter, J. Using pharmacophore models to gain insight into structural binding and virtual screening: an application study with CDK2 and Human DHFR. *J. Chem. Inf. Model.* **2006**, *46*, 728−735.

(10) Rush, T. S., III; Grant, J. A.; Mosyak, L.; Nicholls, A. A shape-based 3-D scaffold hopping method and its application to a bacterial protein-protein interaction. *J. Med. Chem.* **2005**, *48*, 1489−1495.

(11) Grant, J. A.; Gallard, M. A.; Pickup, B. T. A fast method of molecular shape comparison: a simple application of a Gaussian description of molecular shape. *J. Comput. Chem.* **1996**, *17*, 1653−1666.

(12) Güner, O. F.; Henry, D. R. In *Pharmacophore: Perception, Development, and Use in Drug Design;* Güner, O. F., Ed.; International University Line: La Jolla, CA, 2000; pp 193−212.

(13) Wolber, G.; Langer, T. LigandScout: 3D pharmacophores derived from protein-bound ligands and their use as virtual screening filters. *J. Chem. Inf. Model.* **2005**, *45*, 160−169.

(14) Wolber, G.; Dornhofer, A.; Langer, T. Efficient overlay of small molecules using 3-D pharmacophores. *J. Comput.-Aided Mol. Des.* **2006**, *20*, 773−788.

(15) Güner, O.; Clement, O.; Kurogi, Y. Pharmacophore modeling and three dimensional database searching for drug design using Catalyst: recent advances. *Curr. Med. Chem.* **2004**, *11*, 2991−3005.
(16) Kurogi, Y.; Güner, O. F. Pharmacophore modeling and three-dimensional database searching for drug design using Catalyst. *Curr. Med. Chem.* **2001**, *8*, 1035−1055.
(17) Li, J.; Ehlers, T.; Sutter, J.; Varma-O'Brien, S.; Kirchmair, J. CAESAR: A New Conformer Generation Algorithm based on Recursive Build-up and Local Rotational Symmetry Consideration. **2007**, *47*, 1923−1932.
(18) Boström, J. G. J. R.; Gottfries, J. Assessing the performance of Omega with respect to retrieving bioactive conformations. *J. Mol. Graphics Modell.* **2003**, *21*, 449−462.
(19) Wolber, G.; Langer, T. In *Comb*^{i}*Gen: a novel software package for the rapid generation of virtual combinatorial libraries*, 13th European Symposium on Quantitative Structure-Activity Relationships, Duesseldorf, Germany, 2000; Höltje, H.-D., Sippl, W., Eds.; Prous Science, S.A.: Barcelona, Philadelphia, 2001; pp 390−399.
(20) Berman, H. M.; Westbrook, J.; Feng, Z.; Gilliland, G.; Bhat, T. N.; Weissig, H.; Shindyalov, I. N.; Bourne, P. E. The Protein Data Bank. *Nucleic Acids Res.* **2000**, *28*, 235−42.
(21) *Pipeline Pilot, 6.0.2.0*; Scitegic: San Diego, CA, 2006.
(22) Gasteiger, J.; Rudolph, C.; Sadowski, J. Automatic generation of 3D atomic coordinates for organic molecules. *Tetrahedron Comp. Method.* **1990**, *3*, 537−547.
(23) Sadowski, J.; Rudolph, C.; Gasteiger, J. The generation of 3D models of host-guest complexes. *Anal. Chim. Acta* **1992**, *265*, 233−41.
(24) Sadowski, J.; Gasteiger, J.; Klebe, G. Comparison of Automatic Three-Dimensional Model Builders Using 639 X-ray Structures. *J. Chem. Inf. Comput Sci.* **1994**, *34*, 1000−1008.
(25) Edwards, B. S.; Bologa, C.; Young, S. M.; Balakin, K. V.; Prossnitz, E. R.; Savchuck, N. P.; Sklar, L. A.; Oprea, T. I. Integration of virtual screening with high-throughput flow cytometry to identify novel small molecule formylpeptide receptor antagonists. *Mol. Pharmacol.* **2005**, *68*, 1301−1310.
(26) Advanced Seminars in Catalyst. Presented by Accelrys at the 8th European Catalyst User Group Meeting, Innsbruck, Austria, October 1, 2004.
(27) Hirai, H.; Kawanishi, N.; Iwasawa, Y. Recent advances in the development of selective small molecule inhibitors for cyclin-dependent kinases. *Curr. Top. Med. Chem.* **2005**, *5*, 167−179.
(28) Fischer, P. M. The use of CDK inhibitors in oncology: a pharmaceutical perspective. *Cell Cycle* **2004**, *3*, 742−746.
(29) Johnson, G. L.; Lapadat, R. Mitogen-activated protein kinase pathways mediated by ERK, JNK, and p38 protein kinases. *Science* **2002**, *298*, 1911−1912.
(30) Blaschke, F.; Takata, Y.; Caglayan, E.; Law, R. E.; Hsueh, W. A. Obesity, peroxisome proliferator-activated receptor, and atherosclerosis in type 2 diabetes. *Arterioscler., Thromb., Vasc. Biol.* **2006**, *26*, 28−40.
(31) Krovat, E. M.; Fruehwirth, K. H.; Langer, T. Pharmacophore identification, in silico screening, and virtual library design for inhibitors of the human factor Xa. *J. Chem. Inf. Model.* **2005**, *45*, 146−159.
(32) Triballeau, N.; Acher, F.; Brabet, I.; Pin, J.-P.; Bertrand, H.-O. Virtual screening workflow development guided by the "Receiver Operating Characteristic" curve approach. Application to high-throughput docking on metabotropic glutamate receptor subtype 4. *J. Med. Chem.* **2005**, *48*, 2534−2547.
(33) Borodina, Y. V.; Bolton, E.; Fontaine, F.; Bryant, S. H. Assessment of conformational ensemble sizes necessary for specific resolutions of coverage of conformational space. *J. Chem. Inf. Model.* **2007**, *47*, 1428−1437.
(34) Steindl, T. M.; Schuster, D.; Wolber, G.; Laggner, C.; Langer, T. High-throughput structure-based pharmacophore modelling as a basis for successful parallel virtual screening. *J. Comput.-Aided Mol. Des.* **2006**, *20*, 703−715.
(35) Steindl, T. M.; Schuster, D.; Laggner, C.; Langer, T. Parallel screening: a novel concept in pharmacophore modeling and virtual screening. *J. Chem. Inf. Model.* **2006**, *46*, 2146−2157.
(36) Steindl, T. M.; Schuster, D.; Laggner, C.; Chuang, K.; Hoffmann, R. D.; Langer, T. Parallel screening and activity profiling with HIV protease inhibitor pharmacophore models. *J. Chem. Inf. Comput Sci.* **2007**, *47*, 563−571.

CI700024Q